MINERALOGICAL STUDY OF LUNAR DAS IMPACT CRATER USING CHANDRAYAAN-1- MOON MINERALOGICAL MAPPER. A.Karthi[1], Centre for Applied Geology, The Gandhigram Rural Institute-Deemed to be University, Dindigul, Tamilnadu - 624 302, India ([1]karthiatkj@gmail.com)

Introduction: The compositional studies and topographical information will provide the best understanding of the lunar crust evolution [1, 2]. Optical maturity (OMAT) is key to geological marks of the Moon that closely related to its surface maturity of the space environment. The optical maturity parameter is used to derive understanding of the mature and immature index of the lunar surface (higher = immature (fresher), lower = more mature) [3, 4]. Iron and titanium are significant rock-forming elements on the moon and iron and titanium distributions are important for the recognition of lunar mineralogy and crustal evolution [5]. Remotely obtained spectra in the visible near-infrared (VNIR) and shortwave infrared (SWIR) wavelength regions can provide information on the mineralogy abundance of a planetary surface [6]. The present study, focused on elemental composition and spectral charaters of the Das crater in the lunar farside.

Study Area: Das is an impact crater on the far side of the southern Moon (Fig.1 a&b). It is located in latitude of 26°36′S longitude of 136°48′W and it's situted in northwest of the walled plain of Chebyshev. Das is formed in the part of the Copernican system. The crater was named after its Indian discoverer Amil Kumar Das.

Data: Chandrayaan-1 Moon Mineralogical Mapper and Lunar Reconnaissance Orbiter Camera (LROC) – Wide Angle Camera (WAC) and Digital Terrain Modal data were used in the present study. M^3 data from Chandrayaan-1 have provided visible to near-infrared spectral reflectance with high spatial resolutions for capable to investigating the mineralogy of lunar surface [1]. LROC - WAC which has 7-color push-frame camera of the Moon at a uniform resolution of 100m/pixel [12].

Topography: The Das crater has an average depth of 3350m and diameter of 40km (Fig.1 a&b). Topographic information analyzed and obtained with help of LROC-DTM and WAC. The das crater has sharp-edged rim that is not overlaid by any craters and roughly circular in shape, with slightly bulged to the west and northwesten (near to central part). This crater lies at the center of a pale ray system. The inner wall has slumped towards the uneven inner floor, leaving a steeper slope near the rim.

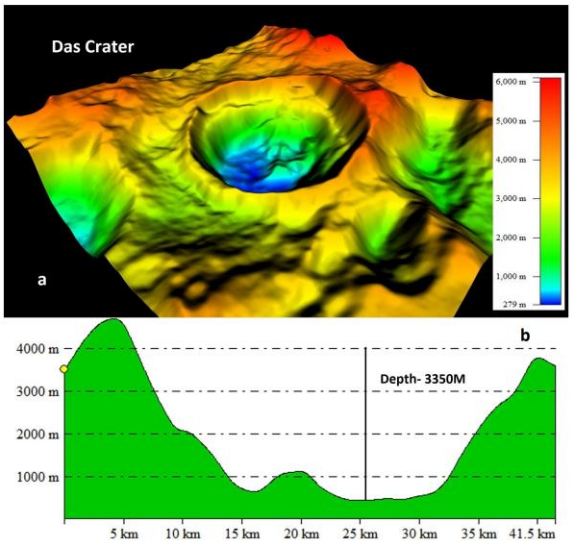

Fig.1. a). Das crater 3D model with elevation measurement and b). Cross section of Das crater.

Results and Discussion:

Das southern and western parts show the low maturity (Near to rim), whereas the high maturity observed at eastern part of the crater (Fig.2). The FeO ranges of the Das crater varies from 0-12%. The western and southern portion of the crater has nearly 8-12% of FeO content (Fig.2). The TiO_2 ranges of the Das crater varies from 0-1.5%, which represents the younger Ti-basalts on the crater (low Ti-basalt-1-5%) [2,7]. The eastern portion of the crater has nearly 1.5% of TiO_2 content (Fig.2). It is observed that, the younger Ti – basalts could have been derived from an olivine – pyroxene source rock at the depth ranging from 200-500km [2,7].

The M^3 Spectral characterization of the das crater shows the different lithological composition (Fig.3). Table 1 shows the spectral characters of the das crater and their compositons. The D1- Spectral characters exhibit a very strong electronic transition absorption near 2000nm and minor moderate absorption varying in 580-640nm due to Fe^{2+} [8], which represents the Mg-rich Spinel absorption. The D2 spectra show the Fe^{2+} weak absorption at 850nm, Plagioclase strong asymmetrical absorption at 1250nm, which may represents the anorthositic composition. The D3 Spectra show the olivine strong asymmetrical absorption at 1050nm, orthopyroxene broad asymmetrical absorption

at 1858nm, which represents the oilvine – pyroxene mixtures [9]. The D4-D6 spectral informations show the Fe^{2+} absorption at 850nm, Cpx strong asymmetrical absorptions at 990-1030nm and 1950-2177nm, plagioclase weak moderate absorption at 1250nm, ilmenite moderate absorptions observed at 1400-1470nm, which may represent the basaltic compositions [10,11].

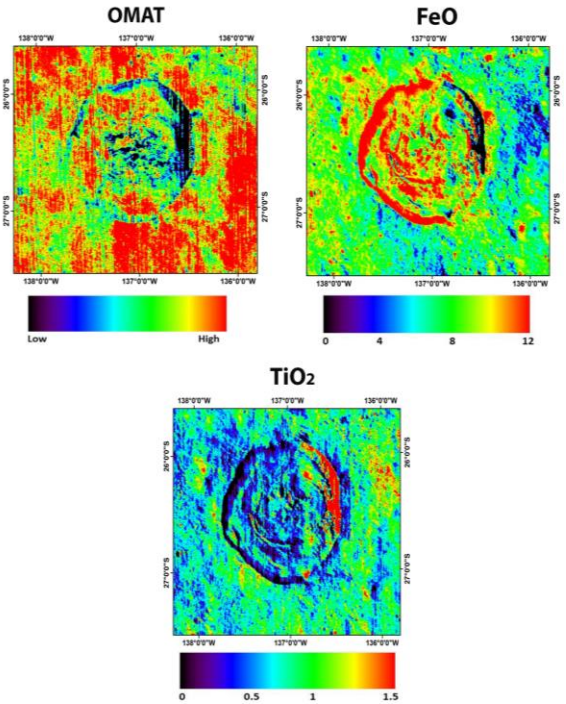

Fig 2. OMAT, FeO and TiO_2 maps of Das crater

Table 1. The spectral characterization of Das crater

Spectra	Absorption (nm)	Causes	Composition
D1	620, 2018	Fe^{2+}, Mg – rich Spinel	Mg-Spinel
D2	850, 1250	Fe^{2+}, Plagioclase	Anorthositic compostion
D3	1050, 1858	Fe-olivine, OPx	Olivine – Pyroxene mixtures
D4	990, 1470, 2177	CPx, Ti-Ilme, CPx	Basaltic Composition
D5	850, 1030, 1400, 1950	Fe^{2+}, CPx, Ti-Ilme, CPx	Basaltic composition
D6	990, 1250, 1450, 2057	CPx, Plg, Ti-Ilm, CPx	Basaltic Composition

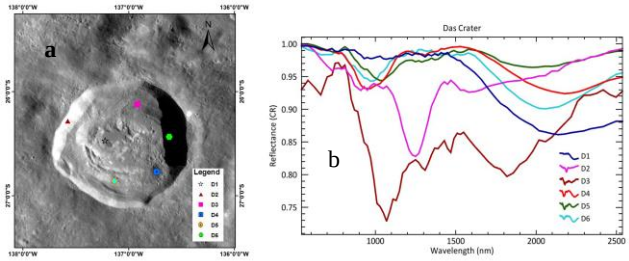

Fig.3. The Das crater spectra obtained locations (a) and their spectral profiles (b)

Summary: In the present study, the elemental mapping, topographical and spectral characterization have been analyzed for the das crater. The FeO (0-12%), TiO_2 (0-1.5%) and OMAT mapping were done. From the results, the spectral characterization of the crater shows the different lithologies such as, Mg-rich-Spinel, Olivine – pyroxene mixtures (which could imply the possibility of relatively thin crust on the Das crater), Anorthositic compostion, and Basaltic compostions.

References:

[1]. Staid MI et al (2011). *J Geophys Res.* doi:10.1029/2010JE003735. [2]. Jin S. et al. (eds.) (2015), *Springer Geophysics*, doi:10.1007/978-3-662-45052-9_2. [3]. Lucey, P.G., (2000b). Journal of *Geophysical Research,* 105(No.E8):20,377-20,386. [4]. Jin, S., et.al, (2013). Advances in Space Research, 52, pg. 285-305. [5]. Lucey, P.G. et al., (2000a) *Journal of Geophysical Research,* 105 (No. E8): 20, 297-20,305. [6]. S. Anbazhagan and S. Arivazhagan., (2009). *Planetary and Space Science*, 57, 1346–1358. [7]. Papike, J.J., (1976). *Rev, Geophys, space physics*, 14,475–540. [8]. C. M. Pieters., et al (2011). *Journal of Geophysical Research*, Vol. 116, E00G08, doi:10.1029/2010JE003727. [9]. Crown, D.A., et al., (1987). *Icarus*, 72 (3), 492–506. https://doi.org/10.1016/0019-1035(87)90047-9. [10]. Isaacson, P. J., (2011). *Journal. Geophys. Res*., 116, E00G11. https://doi.org/10.1029/2010JE003731. [11]. S. Arivazhagan and A. Karthi., (2018). *Planetary and Space Science*, 161 (2018) 41–56. https://doi.org/10.1016/j.pss.2018.06.010. [12]. Robinson, M.S., (2010). *Space Sci Rev*. 150: 81–124. https://doi.org/10.1007/s11214-010-9634-2.

Acknowledgements: The author acknowledges the ISRO, India for financial support from under the CH-1 (AO) Research project- ISRO/SSPO/CH-1/2016-2019.